Borneo Journal of Pharmacy
Vol 8 Issue 2 May 2025
Pages 135 – 148

https://journal.umpr.ac.id/index.php/bjop/article/view/7525
DOI: https://doi.org/10.33084/bjop.v8i2.7525
e-ISSN: 2621-4814

Research Article

Wound Healing Activity of Gel Nanoparticles of *Rhaphidophora pinnnata* Leaves Extract in Male Rats

Fathnur Sani Kasmadi [1*]

Ave Olivia Rahman [2]

Havizur Rahman [1]

Yuliawati [1]

Agung Giri Samudra [3]

[1] Department of Pharmacy, Universitas Jambi, Jambi, Jambi, Indonesia
[2] Department of Medical, Universitas Jambi, Jambi, Jambi, Indonesia
[3] Department of Pharmacy, Universitas Bengkulu, Bengkulu, Bengkulu, Indonesia

*email: fathnursanik@unja.ac.id; phone: +6282380493375

Keywords:
Gel
Nanoparticle
Rhaphidophora pinnata
Wound healing

Abstract

Rhaphidophora pinnata, a plant traditionally recognized for its wound-healing properties, contains active compounds such as megastigmane glycosides and damascenone, known for their anti-inflammatory effects. To enhance efficacy and user comfort, this study focused on developing an *R. pinnata* leaf extract nanoparticle gel. Previous research from our group highlighted the significant wound-healing potential of a conventional *R. pinnata* gel. This present study aimed to evaluate the wound-healing efficacy of a novel *R. pinnata* nanoparticle gel in male Wistar rats, specifically investigating the impact of nanotechnology application. Nanoparticles were successfully formulated via the ionic gelation method, utilizing 0.250 g of *R. pinnata* extract, 0.1% chitosan, 0.2% sodium tripolyphosphate, and 0.5% Tween 80. Characterization revealed an average nanoparticle size of 165.70±42.76 nm with a zeta potential of 22.0±1.83 mV. The wound-healing efficacy was assessed across five treatment groups: a positive control (Bioplasenton®), a plain gel base (Formula 0), and nanoparticle gels at 0.5% (Formula I), 1% (Formula II), and 1.5% (Formula III) extract concentrations. Statistical analysis using one-way ANOVA ($p < 0.05$) demonstrated a significant difference in incision wound healing across the groups. Formula III, containing 1.5% *R. pinnata* nanoparticle extract, exhibited the most superior wound-healing effect, achieving 100% inhibition by day 14, elevated hydroxyproline levels (59 µg/mL), and histologically confirmed excellent skin tissue repair. Formulas II and I followed in efficacy. These compelling findings underscore the significant potential of utilizing nanotechnology in the development of topical preparations for accelerated and effective wound healing.

Received: July 7th, 2024
1st Revised: August 30th, 2024
Accepted: May 22nd, 2025
Published: May 30th, 2025

INTRODUCTION

Wound healing is a complex biological process essential for restoring the integrity of damaged tissues, typically involving intricate stages of inflammation, proliferation, and remodeling. Wounds, characterized by cellular and tissue structural disorders, can range from superficial epidermal damage to extensive injury involving subcutaneous tissue, tendons, muscles, nerve vessels, parenchymal organs, and bones. Various etiologies, including chemical, physical, and thermal insults, can lead to wound formation. The initial inflammatory phase, a vital pathological response to injury, involves the localized accumulation of blood cells and plasma fluid, crucial for clearing debris and initiating repair processes[1]. In Indonesia, traditional herbal medicine plays a significant role in wound management, with local communities commonly employing poultices of medicinal plants on affected skin.

How to cite: Kasmadi FS, Rahman AO, Rahman H, Yuliawati, Samudra AG. Wound Healing Activity of Gel Nanoparticles of Rhaphidophora pinnnata Leaves Extract in Male Rats. Borneo J Pharm. 2025;8(2):135-48. doi:10.33084/bjop.v8i2.7525

Among these traditional remedies, *Rhaphidophora pinnata* leaves are widely recognized for their diverse therapeutic benefits, particularly in wound and inflammation healing. This plant is rich in secondary metabolites, including alkaloids, flavonoids, saponins, tannins, steroids, and phenolics, which are key contributors to its reported wound-healing properties. Pharmacological studies have substantiated its efficacy as an anti-inflammatory and wound-healing agent. Our previous investigations with *R. pinnata* leaf extract, formulated in a gel, demonstrated that a 15% extract concentration yielded optimal wound-healing efficacy[2]. Furthermore, the extract's wound-healing potential is supported by its capacity to inhibit cancer cell growth through mechanisms involving increased apoptosis, angiogenesis, and antiproliferative activity. Research by Pan *et al*.[3] specifically identified megastigmane glycosides, gusanlungionoside, citroside, phenyl alcohol glycoside, galactopyranoside, aglycon damascenone, megastigmatrienone, 3-hydroxy-β-damascenone, and 3-oxo-7,8-dihydro-α-iono as active compounds responsible for its anti-inflammatory effects. Pharmacological analyses confirm that these compounds inhibit LPS-stimulated induction of pro-inflammatory cytokines and leukocyte adhesion molecules, such as TNF-α, IL-1β, IL-8, and COX-2. These findings are further corroborated by research conducted by Tarigan *et al*[4].

Recent advancements in pharmaceutical science highlight the promising role of nanotechnology in drug delivery. Nanoparticles, characterized by their exceptionally small size (1-1000 nm), serve as effective carriers for active compounds, enabling improved dissolution and encapsulation of therapeutic agents[5,6]. Pharmaceutical preparations utilizing nanoparticles offer notable advantages, such as reducing the frequency of drug administration and achieving significant therapeutic effects at lower doses[7]. Moreover, the formulation of nanoparticles represents a sophisticated modification of traditional topical preparations, capable of mitigating systemic side effects[8]. Topical drug administration allows for localized action, bypasses first-pass metabolism, and offers a safe and comfortable delivery route for injured and inflamed skin[9]. Consequently, developing nanoparticle-based gel preparations of plant extracts is a promising approach to enhance the pharmacokinetic and pharmacodynamic profiles of phytopharmaceuticals[10]. Building upon these challenges and opportunities, this study aims to investigate the wound-healing effects of varying *R. pinnata* extract nanoparticle gel formulations in white male rats. Specifically, we seek to analyze how changes in extract particle size within these nanoparticle formulations influence their efficacy in promoting wound healing.

MATERIALS AND METHODS

Materials

Fresh leaves of *R. pinnata* (syn. *Epipremnum pinnatum*) were collected from Mendalo, Jambi, Indonesia, in June 2021. Botanical identification was performed by a taxonomist from the Department of Biology, Faculty of Mathematics and Natural Sciences, Universits Andalas, where a voucher specimen (250/K-ID/ANDA/VI/2021) has been deposited. All chemical reagents and pharmaceutical-grade materials were obtained from reputable suppliers. These included: distilled water, 2 N H_2SO_4, Dragendorff's reagent, Mayer's reagent, Wagner's reagent, Bioplacenton (PT. Kalbe Farma), sodium tripolyphosphate (STPP), carbopol, tween, carrageenan, glycerin, propylene glycol, triethanolamine, methylparaben, propylparaben, ethanol (PT. Brataco), and Veet (PT. Reckitt Benckiser Indonesia).

Methods

Rhaphidophora pinnata leaf extraction

Rhaphidophora pinnata leaves were subjected to maceration using 70% ethanol as the solvent. Briefly, the dried simplicia powder was placed into an appropriate container, and 70% ethanol was added until the powder was fully submerged. The container was then sealed and allowed to macerate for 24 hours, with the solvent being replaced two additional times at 24-hour intervals to ensure optimal extraction. Following maceration, the mixture was filtered to separate the solid residue from the liquid macerate. The resulting macerate was subsequently concentrated under reduced pressure at 40°C using a rotary evaporator until complete dryness, yielding the crude ethanolic extract.

Phytochemical screening

Phenolics: Qualitative analysis for phenolic compounds was conducted by dissolving 0.5 g of the extract in 10 mL of ethanol in a test tube. Subsequently, 2-3 drops of 1% $FeCl_3$ solution were added. The formation of a dark blue-black coloration indicated the presence of phenolic compounds.

Alkaloids: For the qualitative analysis of alkaloids, 0.5 g of the extract was accurately weighed and transferred into a test tube. The extract was then dissolved in 5 mL of 2 N HCl and subsequently divided into two equal aliquots. Mayer's reagent was added to the first aliquot, while Dragendorff's reagent was added to the second. The formation of a white precipitate upon the addition of Mayer's reagent indicated a positive result for alkaloids. Conversely, a positive result with Dragendorff's reagent was evidenced by the appearance of a light brown to yellow precipitate.

Flavonoids: The presence of flavonoids in the extract was qualitatively assessed using the modified Wilstätter test. Briefly, 0.5 g of the prepared extract was accurately weighed and completely dissolved in 5 mL of ethanol. From this solution, a 1 mL aliquot was transferred to a clean test tube. Subsequently, two to three small pieces of magnesium turnings were added, followed by the careful addition of 2-4 drops of concentrated HCl. The mixture was gently agitated and observed for any color changes. A positive result, indicating the presence of flavonoids, was evidenced by a visible color change from orange to reddish within the solution.

Saponins: To detect the presence of saponins, 0.5 g of the extract was accurately weighed into a test tube. Ten milliliters of hot distilled water were then added, and the mixture was allowed to cool before being vigorously shaken. The formation of a persistent foam layer, 1-10 cm in height, which remained stable for at least 10 minutes and did not dissipate upon the addition of 2 N HCl, was indicative of saponins.

Tannins: Briefly, 0.5 g of the dried extract was accurately weighed and completely dissolved in 5 mL of 95% ethanol. From this prepared solution, a 1 mL aliquot was transferred to a test tube, and subsequently, 2-3 drops of 1% $FeCl_3$ solution were added, followed by the addition of gelatin solution. The observation of a distinct color change to dark blue or greenish-black within the solution was considered a positive indication for the presence of tannins.

Steroids and terpenoids: The presence of steroids and terpenoids in the extract was determined using the Liebermann-Burchard test. Briefly, 50 mg of the extract was accurately weighed into a test tube. To this, 10 drops of glacial acetic acid were added, followed by 2 drops of H_2SO_4. The mixture was then gently shaken. The development of a distinct greenish-blue ring at the interface indicated the presence of steroids, while a reddish-orange ring suggested the presence of terpenoids.

Total phenolic content

The total phenolic content of the *R. pinnata* leaves ethanol extract was quantitatively determined using the Folin-Ciocalteu spectrophotometric method, employing a UV-Vis spectrophotometer. For extract preparation, approximately 0.125 g of the dried extract was accurately weighed and dissolved in 25 mL of absolute ethanol. The mixture was then stirred for 30 minutes using a magnetic stirrer to achieve a working concentration of 500 ppm. For the assay, 1 mL of this extract solution was combined with 5 mL of Folin-Ciocalteu reagent and allowed to react for 8 minutes. Subsequently, 4 mL of 1% NaOH solution was added, and the mixture was incubated in the dark for 1 hour. Absorbance was then measured at a maximum wavelength of 730 nm. A standard curve was generated using gallic acid solutions at concentrations of 5, 15, 30, and 50 ppm. The total phenolic content of the extract was calculated from the linear regression equation derived from the gallic acid standard curve and expressed as mg of gallic acid equivalent per g of extract (mg GAE/g).

Total flavonoid content

The total flavonoid content of the ethanolic extract of *R. pinnata* leaves was quantified spectrophotometrically using the $AlCl_3$ method, with measurements performed on a UV-Vis spectrophotometer. For sample preparation, 0.20 g of the extract was accurately weighed, transferred to an Erlenmeyer flask, and thoroughly dissolved in 25 mL of absolute ethanol. The solution was then stirred for 30 minutes using a magnetic stirrer, followed by filtration into a 25-mL volumetric flask. The volume was subsequently made up to the mark with absolute ethanol. For the reaction, a 0.5 mL aliquot of the test solution was pipetted and mixed with 1.5 mL of absolute ethanol, 0.1 mL of 10% $AlCl_3$ solution, and 0.1 mL of sodium acetate solution. Distilled water was then added to the mixture to achieve a final volume of 10 mL. Following a 30-minute incubation period at room temperature, the absorbance of the reaction mixture was measured at 440 nm. A standard curve was generated using varying concentrations of quercetin (25, 50, 75, and 100 µg/mL). The total flavonoid content in the extract was calculated from the linear regression equation derived from the standard curve and expressed as mg of quercetin equivalents (mg QE/g).

Preparation of nanoemulsion from Rhaphidophora pinnata leaf extract

The nanoemulsion containing *R. pinnata* leaf extract was prepared following a modified method adapted from Samudra *et al*[11,12]. Briefly, a 0.1% chitosan solution was prepared by dissolving 0.1 g of chitosan in 100 mL of 1% acetic acid solution under continuous magnetic stirring. Concurrently, a 0.2% STPP solution was formulated by dissolving 0.2 g of STPP in 100 mL of deionized water with magnetic stirring. Separately, a 0.5% Tween 80 solution was prepared by dissolving 0.5 mL of Tween 80 in 100 mL of deionized water. For the nanoemulsion formation, 2.5 g of *R. pinnata* leaf extract was thoroughly mixed with 18 mL of the 0.1% chitosan solution using a magnetic stirrer at 2,500 rpm for 30 minutes. Subsequently, 9 mL of the 0.2% STPP solution was added dropwise to the mixture, which was continuously stirred at 2,500 rpm for another 30 minutes. Finally, 3 mL of the 0.5% Tween 80 solution was added dropwise, and the mixture was stirred under the same conditions (2,500 rpm for 30 minutes) until a homogeneous nanoparticle emulsion solution was formed.

Characterization of nanoemulsions

The physical characteristics of the prepared nanoemulsions were thoroughly assessed using a HORIBA SZ-100 nanoparticle analyzer. The average hydrodynamic diameter of the nano-dispersed particles was determined by dynamic light scattering (DLS). For these measurements, samples were judiciously diluted at a ratio of 1:5 with deionized water to prevent the occurrence of multiple scattering events, which could otherwise distort the results. All DLS measurements were conducted at a controlled temperature of 25°C. In parallel, the zeta potential of the nanoemulsion particles, a critical indicator of colloidal stability, was measured using the electrophoretic mobility distribution of particles. This was achieved through the laser Doppler velocimetry technique, which quantifies the movement of charged particles in an electric field. A precise sample volume of 100 µL was carefully introduced into the instrument for each measurement. Consistent with the particle size analysis, zeta potential measurements were also performed at 25°C[13,14].

Gel formulation

The nanoemulgel formulations containing *R. pinnata* leaves extract were prepared according to the compositions detailed in **Table I**. The method involved a systematic two-phase approach to ensure homogeneity and stability. First, the aqueous gel base was prepared by accurately weighing Carbopol and slowly dispersing it in distilled water within a porcelain mortar. The mixture was then allowed to swell completely to achieve a clear, viscous dispersion. Simultaneously, methylparaben, serving as a preservative, was dissolved in glycerin in a separate beaker, ensuring complete dissolution through gentle stirring. Concurrently, the *R. pinnata* leaves extract, previously prepared as nanoparticles, was accurately weighed for each desired concentration and carefully triturated in a clean mortar until a smooth, uniform consistency was achieved. Propylene glycol, acting as a humectant and permeation enhancer, was then gradually incorporated into the nanoparticle mixture with continuous trituration to form a homogeneous preparation. Finally, the swollen Carbopol dispersion was carefully transferred to the mortar containing the extract-propylene glycol mixture. Triethanolamine (TEA) was then added dropwise with continuous trituration until a gel structure was formed, indicating neutralization of the Carbopol and the desired consistency. The previously prepared mixture of glycerin and dissolved methylparaben was subsequently incorporated into this gel base and thoroughly mixed until complete integration and homogeneity were achieved. Any remaining volume of distilled water was then added to attain the final desired weight, followed by thorough mixing to ensure a uniform nanoemulgel.

Table I. *Rhaphidophora pinnata* leaf extract nanoparticle gel formulation.

Materials	Concentration (%)				Description
	F0	FI	FII	FIII	
Rhaphidophora pinnata leaf nanoparticle extract	0	0.5	1	1.5	Active substance
Carbopol	1	1	1	1	Gel base
Glycerin	5	5	5	5	Humectant
Propylene glycol	10	10	10	10	Penetration Enhancer
TEA	1	1	1	1	Buffer
Methylparaben	0.2	0.2	0.2	0.2	Preservative
Distilled water ad	100	100	100	100	Solvent (q.s. to 100%)

Note: F0: Plain gel base (negative control); FI: Nanoemulgel containing 0.5% *R. pinnata* nanoparticle extract; FII: Nanoemulgel containing 1% *R. pinnata* nanoparticle extract; FIII: Nanoemulgel containing 1.5% *R. pinnata* nanoparticle extract.

Evaluation of gel preparations

The freshly prepared gel formulations underwent a comprehensive evaluation at weeks 0, 1, 2, 3, and 4 of storage at room temperature. This assessment included the examination of organoleptic properties, homogeneity, pH, spreadability, adhesion, and viscosity. Organoleptic evaluation involved visual observation of the gel's color, odor, and physical form throughout the storage period. Homogeneity was assessed by applying a small amount of the preparation onto a transparent glass surface and visually inspecting for any inconsistencies or particulate matter[15]. For pH measurement, a calibrated pH meter was utilized by immersing its reference and glass electrodes directly into the ointment[16]. Spreadability was determined by placing 0.5 g of the gel preparation between two round glass plates. After one minute, a 150 g weight was applied to the top plate for another minute. The diameter of the spread gel was then measured to quantify its spreadability. Adhesion was evaluated by placing 0.25 g of the gel between two glass slides. A 1 kg load was applied for 5 minutes, after which the slides were separated using a hook connected to 100 g weights, and the time required for complete separation was recorded. Finally, viscosity was measured using a Brookfield viscometer (spindle number 6, 50 rpm) at room temperature, adhering strictly to the manufacturer's standard operating procedures[17].

Wound healing test with nanoparticle gel extract of Rhaphidophora pinnata leaves

The wound healing activity of the *R. pinnata* nanoparticle extract gel was evaluated using male Wistar rats (200-250 g). To ensure optimal experimental conditions and minimize potential confounding factors from inter-animal interactions, each rat was housed individually in a dedicated cage. All animal procedures were conducted in strict accordance with ethical guidelines, and approval was obtained from the Ethics Committee of the Faculty of Medicine, Universitas Tadulako (Number: 3096/UN28.1.20/KL/2021).

Prior to wound induction, the dorsal area of each rat was depilated using Veet® hair removal cream, followed by sterilization with 70% ethanol. Anesthesia was induced via intraperitoneal injection of ketamine hydrochloride (50 mg/kg BW) and xylazine hydrochloride (10 mg/kg BW). A standardized full-thickness incision wound, measuring 3 cm in length and 0.3 cm in depth, was then meticulously created on the dorsolateral region of the back using a sterile scalpel blade (number 12)[18]. Rats were randomly assigned to one of five treatment groups, with five animals per group:

Positive control: Bioplacenton® (a commercially available wound healing gel; positive control).

Formula 0: Plain gel base (negative control).

Formula I: Nanoemulgel containing 0.5% *R. pinnata* nanoparticle extract.

Formula II: Nanoemulgel containing 1% *R. pinnata* nanoparticle extract.

Formula III: Nanoemulgel containing 1.5% *R. pinnata* nanoparticle extract.

Each treatment (0.3 g) was topically applied to the wound site twice daily for 14 consecutive days. Wound healing progression was monitored over this 14-day period by assessing the percentage of wound closure. The percentage of wound healing was calculated using **Equation 1**, which represents the reduction in wound area relative to the initial wound size.

$$\text{Percentage of wound contraction (\%)} = \frac{\text{Initial wound size} - \text{specific day wound size}}{\text{Initial wound size}} \; x \; 100\% \qquad [1]$$

Determination of hydroxyproline levels

To assess collagen formation within the healing wounds, skin biopsies were systematically collected from the experimental animals. Biopsies were taken at the initiation of the treatment (Day 0) and subsequently on Day 15. Prior to tissue collection, animals were humanely anesthetized via intraperitoneal injection of a combination of ketamine hydrochloride (50 mg/KgBW) and xylazine hydrochloride (10 mg/KgBW). As hydroxyproline is a fundamental constituent of collagen, its quantification serves as a reliable indicator of collagen content in the skin. Following biopsy, the excised skin tissue samples were dried in an oven at 60°C for 12 hours. The dried tissue was then subjected to acid hydrolysis using 6 N HCl at 110°C for 24 hours to liberate hydroxyproline. The resulting hydrolysate was meticulously neutralized to pH 7 using a buffer system consisting of 0.2 M NH_4Cl, 0.2 M NH_4OH, and 2.5 N NaOH. Subsequently, a series of reagents were added to the neutralized hydrolysate: 1 mL of 0.01 N $CuSO_4$, 1 mL of 2.5 N NaOH, and 1 mL of 6% H_2O_2. This mixture was stirred and heated at 80°C for 5 minutes. After cooling, 4 mL of 3 M H_2SO_4 and 2 mL of 5% 2-dimethylamino benzaldehyde were added. The solution was then heated at 70°C for 16 minutes, cooled, and the absorbance was measured at 560 nm using a UV-Vis spectrophotometer.

Skin histology

On day 15 of the study, skin samples were harvested from the animal subjects for subsequent histological examination. Prior to tissue collection, animals were humanely anesthetized via euthanasia using a ketamine-xylazine anesthetic cocktail (0.1 mL/100 g BW, containing 4-10 mg ketamine and 0.5-1.3 mg xylazine). Following euthanasia, skin tissue was carefully excised. The harvested skin organs underwent a standardized histological processing protocol to assess the formation of skin epithelial cells, neovascularization, and collagen deposition. This protocol involved initial washing with 0.9% NaCl, followed by precise weighing of the tissue samples. Tissues were then fixed in a 10% formalin solution. Dehydration was performed through a graded series of alcohol (70%, 80%, 90%, 95% for 24 hours each, followed by three changes of 100% absolute alcohol for one hour per change). Subsequently, tissues were cleared in xylol (three changes, one hour per change) before paraffin infiltration. The processed organs were embedded in paraffin blocks, and sections of 4-5 µm thickness were prepared. These sections were then stained with Hematoxylin and Eosin (H&E) for microscopic observation. Prepared slides were systematically labeled, and their morphological characteristics were meticulously analyzed.

Data analysis

Data analysis was performed using a two-pronged approach to comprehensively interpret the research findings. Firstly, descriptive statistics were employed to summarize and characterize the collected data, providing insights into central tendencies and variability of key variables. This allowed for a clear understanding of the sample characteristics and the distribution of observations. Secondly, to test for statistically significant differences between experimental groups, a one-way ANOVA was conducted. All inferential statistical analyses, including the ANOVA, were performed with a predetermined significance level of α=0.05, corresponding to a 95% confidence level.

RESULTS AND DISCUSSION

Our phytochemical screening of the *R. pinnata* leaf extract revealed the presence of several key secondary metabolites, including flavonoids, alkaloids, saponins, tannins, steroids, and phenols (**Table II**). These findings are consistent with previous studies that have extensively characterized the chemical profile of this plant. For instance, prior investigations have identified specific compounds such as pyridine, 3,4-dihydroxybenzyl alcohol, ester, isobutyl amine, and urea within *R. pinnata*. The observed abundance of phenolic compounds in our extract aligns with these reports, suggesting a significant contribution to its potential bioactivity. Furthermore, a comprehensive study by Pan *et al*.[3] has highlighted the presence of diverse chemical constituents in *R. pinnata*, including megastigmane glycosides (such as gusanlungionoside and citroside), phenyl alcohol glycosides (e.g., phenyl methyl 2-O(6-O-rhamnosyl)-β-D-galactopyranoside), and various aglycones like damascenone, megastigmatrienone, 3-hydroxy-β-damascenone, and 3-oxo-7,8-dihydro-α-iono.

Table II. Phytochemical screening results.

Phytochemical test	Results
Phenolics	+
Alkaloids	+
Flavonoids	+
Saponins	+
Tannins	+
Steroids	+
Terpenoids	-

The total phenolic content of the *R. pinnata* ethanolic extract was determined using the Folin-Ciocalteu spectrophotometric method with gallic acid as the reference standard. This technique relies on the principle that phenolic compounds react with the Folin-Ciocalteu reagent in an alkaline environment to form a distinct blue complex. The intensity of this complex, directly proportional to the phenolic concentration, is then quantified spectrophotometrically. Gallic acid was chosen as the comparative standard due to its stability, commercial availability, and its effective complex formation with the Folin-Ciocalteu reagent, facilitated by its hydroxyl groups and conjugated double bonds within the benzene ring. For the assay, four different concentrations of the extract were analyzed spectrophotometrically at a maximum wavelength of 730 nm[19-21]. A linear regression equation of $y = 0.0103x + 0.0992$ with a high coefficient of determination (R^2) of 0.9996 was generated

from the calibration curve. Based on these analyses, the ethanolic extract of *R. pinnata* was found to contain a total phenolic content of 2.37 mg GAE/100 g extract.

The total flavonoid content was assessed using the UV-visible spectrophotometry method, employing a colorimetric assay with $AlCl_3$ reagent at a wavelength of 450 nm. This method leverages the ability of $AlCl_3$ to form acid-resistant complexes with the hydroxyl group adjacent to the ketone group, or with the ortho-hydroxyl groups, present in flavonoids. Quercetin was selected as the reference standard for comparison, as it is a well-characterized flavonol possessing a ketone group at C-4 and hydroxyl groups at C-3 or C-5, enabling effective color complex formation with $AlCl_3$[19,20,22]. The analysis yielded a linear regression equation of $y = 0.0096x - 0.243$ with R^2 of 0.9947. Our findings indicate that the ethanolic extract contains 0.90 mg QE/100 g extract.

The nanoemulsion in this study was formulated using the ionic gelation method, a technique characterized by a cross-linking process between polyelectrolytes in the presence of multivalent ion pairs[23,24]. Chitosan, a biopolymer derived from chitin (poly(b-1/4)-2-amino-2-deoxy-D-glucopyranose), was utilized as the primary carrier. Chitosan is frequently employed in nanotechnology due to its ability to enhance drug stability[25,26]. Sodium tripolyphosphate served as the crosslinker agent, chosen for its negative charge which facilitates strong interactions with positively charged polycations, making it more effective than other polyanions like sulfate or citrate. In this method, chitosan acts as a polycation carrying multivalent positive ions, which then interact with the negatively charged STPP. Variations in the ionic concentration directly influence the physical properties of the resulting nanoparticles[26]. Furthermore, Tween 80 was incorporated as a surfactant to stabilize the particle diameter and prevent aggregation[12].

The characterization of nanoparticles derived from *R. pinnata* leaf extract yielded a particle size of 165.7 ± 42.76 nm. This size range is considered optimal for drug delivery applications, as literature suggests that nanoparticles between 50-300 nm are highly effective for cellular uptake [19–21]. This finding aligns with research by Hoshyar *et al.*[27], which demonstrated that drug-laden particles smaller than 1000 nm exhibit 2.5 to 250 times greater absorption compared to larger particles. Further supporting the favorable characteristics of these nanoparticles are the polydispersity index (PDI) of 0.562 ± 0.023 and a zeta potential of 22 ± 1.83 mV. The zeta potential is a crucial measure of the electric charge at the surface of colloidal particles[28-30]. It quantifies the difference in electrical charge between the granules and the dispersed colloidal particle layer, directly correlating with nanoparticle stability. Higher repulsive forces between particles, indicated by a greater zeta potential, contribute to enhanced nanosystem stability[31]. An optimal zeta potential value is typically considered to be near ±30 mV, which contributes to greater colloidal stability. The polydispersity index (PDI), ranging from 0 to 1, reflects the homogeneity of the sample, with a lower value indicating a more uniform particle size distribution and improved long-term stability of the nanoemulsion[32].

The preparation of chitosan nanoparticles via the ionic gelation method leverages chitosan's polycationic nature. Its multivalent positive ions readily interact with the negative ions of STPP. This interaction involves a deprotonation reaction where hydroxyl ions from STPP ionically compete with the $-NH^{3+}$ groups in chitosan, forming an ionic gel. Sodium tripolyphosphate was specifically chosen as the crosslinker due to its potent negative charge, which facilitates stronger interactions compared to other polyanions like sulfate and citrate. Moreover, its non-toxic nature makes STPP highly suitable for various biomedical applications[33].

The physicochemical properties of the *R. pinnata* leaf extract gel formulations were systematically evaluated over a four-week period, with observations made at Weeks 0, 1, 2, 3, and 4, as summarized in **Table III**. Our findings indicate that the *R. pinnata* leaf extract nanoparticle gels across all tested formulations exhibited excellent organoleptic stability, showing no significant changes in appearance, color, or odor throughout the four-week observation period. Furthermore, critical parameters such as pH, spreadability, and adhesion consistently remained within acceptable ranges for topical gel preparations. Specifically, the pH values were maintained within the desirable physiological range of 6 to 7, ensuring skin compatibility. The spreadability of the gels was optimal, ranging from 5 to 7 cm, which facilitates ease of application. Adhesion properties were also satisfactory, with values consistently between 1 and 3 seconds, suggesting good retention on the skin surface. This remarkable stability, particularly the consistent physicochemical profile, is likely attributed to the relatively low concentration of the *R. pinnata* extract incorporated into the gel formulations. This low extract content appears to maintain the structural integrity and cohesive forces among the carbopol molecules, thereby ensuring the overall stability of the gel matrix throughout the study period[2,34].

Table III. Evaluation results of *R. pinnata* leaf nanoparticle extract gel preparations.

Formula	Observation	Day 0	Day 7	Day 14	Day 21	Day 28
F0	Organoleptic					
	a. Color	Clear	Clear	Clear	Clear	Clear
	b. Smell	Typical	Typical	Typical	Typical	Typical
	c. Form	Thick	Thick	Thick	Thick	Thick
	Homogeneity	Homogeneous	Homogeneous	Homogeneous	Homogeneous	Homogeneous
	pH	6.41 ± 0.05*	6.83 ± 0.03*	6.25 ± 0.02*	6.46 ± 0.08*	6.7 ± 0.02*
	Adhesion	10 ± 5.29*	15.2 ± 7.63*	13.7 ± 4.07*	9.58 ± 4.05*	5.71 ± 2.55*
	Spreadability	3.45 ± 0.74*	3.69 ± 0.69*	4.12 ± 0.48*	3.91 ± 2.26*	4.36 ± 1.44*
FI	Organoleptic					
	a. Color	Light yellow	Light yellow	Light yellow	Light yellow	Light yellow
	b. Smell	Typical	Typical	Typical	Typical	Typical
	c. Form	Thick	Thick	Thick	Thick	Thick
	Homogeneity	Homogeneous	Homogeneous	Homogeneous	Homogeneous	Homogeneous
	pH	6.62 ± 0.18*	6.16 ± 0.04*	6.32 ± 0.02*	6.53 ± 0.02*	6.49 ± 0.01*
	Adhesion	2.49 ± 0.50*	2.12 ± 0.29*	2.07 ± 0.18*	2.94 ± 0.85*	2.81 ± 0.56*
	Spreadability	6.18 ± 0.65*	6.7 ± 1.43*	6.9 ± 0.64*	6.3 ± 4.41*	6.8 ± 0.93*
FII	Organoleptic					
	a. Color	Light brown	Light brown	Light brown	Light brown	Light brown
	b. Smell	Typical	Typical	Typical	Typical	Typical
	c. Form	Thick	Thick	Thick	Thick	Thick
	Homogeneity	Homogeneous	Homogeneous	Homogeneous	Homogeneous	Homogeneous
	pH	6.62 ± 0.09*	6.2 ± 0.26*	6.67 ± 0.02*	6.43 ± 0.03*	6.51 ± 0.06*
	Adhesion	1.49 ± 0.69*	1.98 ± 0.35*	1.73 ± 0.40*	1.95 ± 0.30*	1.64 ± 0.40*
	Spreadability	6 ± 0.68*	5.8 ± 0.81*	5.43 ± 0.22*	6.8 ± 4.46*	6.4 ± 2.46*
FIII	Organoleptic					
	a. Color	Greenish brown	Greenish brown	Greenish brown	Greenish brown	Greenish brown
	b. Smell	Typical	Typical	Typical	Typical	Typical
	c. Form	Thick	Thick	Thick	Thick	Thick
	Homogeneity	Homogeneous	Homogeneous	Homogeneous	Homogeneous	Homogeneous
	pH	6.84 ± 0.06*	6.30 ± 0.30*	7 ± 0.20*	6.83 ± 0.15*	6.7 ± 0.01*
	Adhesion	1.91 ± 0.16*	1.86 ± 0.10*	1.86 ± 0.10*	1.89 ± 0.03*	1.98 ± 0.04*
	Spreadability	6.8 ± 0.65*	6.41 ± 0.62*	6.9 ± 0.44*	6.5 ± 1.42*	6.3 ± 1.72*

Note: (*) indicates the data meets the requirements for evaluating topical preparations.

To evaluate the wound-healing efficacy of the developed nanoemulgel formulations, an incision wound model was employed in this study. An incision wound, defined as a disruption of skin tissue continuity resulting from injury or surgical intervention, was chosen due to its widespread occurrence in both clinical settings and daily life. This model's relevance to common skin damage scenarios makes the evaluation highly pertinent for developing a natural-based wound therapy potentially applicable by both the general public and healthcare professionals[35].

The wound length was meticulously measured daily over a 14-day observation period. Statistical analysis revealed a significant difference in wound healing rates among the various treatment groups ($p < 0.05$). Further post-hoc tests identified Formula III, containing a 1.5% nanoparticle extract concentration, as the most effective gel formulation. This superior performance was evidenced by a remarkable 100% wound healing percentage achieved by day 14 of observation, followed by Formulas II and I, respectively (**Figure 1**). For comparative purposes, Bioplacenton® was utilized as a positive control. Bioplacenton® is a commercially available wound healing agent comprising active placenta extract and neomycin sulfate. The placenta extract functions as a "biogenic stimulator," playing a crucial role in accelerating cellular regeneration and the overall wound healing process. In parallel, neomycin sulfate provides antibiotic action, effectively combating microbial proliferation at the wound site, thereby preventing infection[2].

The histopathological analysis of rat skin tissue aimed to elucidate the reparative effects of *R. pinnata* extract nanoparticle gel on wound damage. Observations revealed a marked difference in tissue regeneration across treatment groups. Specifically, the negative control group exhibited a diminished capacity for epithelial tissue formation and a reduction in collagen synthesis, indicating impaired wound healing. In contrast, the groups treated with the *R. pinnata* extract nanoparticle gel demonstrated robust epithelial tissue regeneration and a significant increase in collagen deposition. This resulted in complete epidermal coverage of the skin, signifying successful wound repair (**Figure 2**).

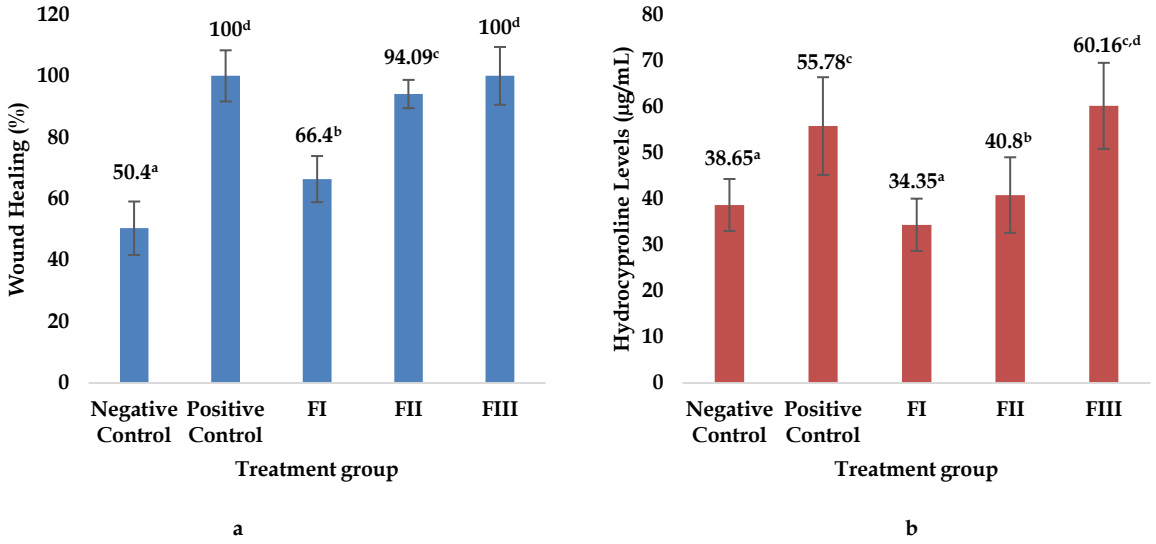

Figure 1. Wound healing (**a**) and hydroxyproline levels (**b**) on day 14 ± SD. Different lowercase superscripts indicate significant differences ($p < 0.05$).

Previous research has extensively documented the anti-inflammatory properties of *R. pinnata* leaf extract[3,4]. Furthermore, a 15% concentration of *R. pinnata* leaf extract in gel form has been shown to exhibit both good stability and a remarkable 100% wound healing potential after 14 days of treatment. Our current findings demonstrate that reformulating this extract into nanoparticles significantly enhances its topical drug delivery, allowing for a remarkably lower effective dose of 1.5% to achieve 100% wound healing within the same 14-day treatment period. This enhanced efficacy at a reduced concentration aligns with the principles highlighted by Hajialyani *et al.*[36], who noted that nanoparticle-sized preparations increase drug penetration into skin tissue, thereby improving wound healing efficiency and enabling a reduction in the active ingredient concentration.

The immense potential of natural materials in wound management and treatment has been recognized since ancient times. The widespread historical use of plants for wound healing underscores the ease of raw material acquisition at low costs. Consequently, numerous phytopharmaceutical laboratories are actively engaged in researching the active compounds within plants that possess medicinal value, contributing to a growing body of scientific literature on natural remedies[37].

Research on the isolation of compounds from *R. pinnata* has identified several significant constituents, including megastigmane glycosides, gusanlungionoside, citroside, phenyl alcohol glycoside phenyl methyl 2-O(6-O-rhamnosyl)-β-D-galactopyranoside, aglycon damascenone, megastigmatrienone, 3-hydroxy-β-damascenone, and 3-oxo-7,8-dihydro-α-iono. Many of these compounds are known for their antioxidant activity, which may fundamentally contribute to the observed pharmacological properties. For instance, analysis has demonstrated that *R. pinnata* inhibits LPS-stimulated induction of mRNAs encoding for pro-inflammatory cytokines and leukocyte adhesion molecules, such as TNF-α, IL-1β, IL-8, and COX-2[3].

Beyond the enhanced particle size achieved through nanoformulation, the observed wound healing effect is further supported by the presence of key secondary metabolites, including alkaloids, flavonoids, saponins, steroids, and tannins. Alkaloids are known to reduce cytokine production, thereby mitigating inflammation during the wound healing process[38]. Flavonoids, on the other hand, play a crucial role in inhibiting the activity of cyclooxygenase and lipoxygenase enzymes, and both acts to suppress the biosynthesis of prostaglandins and leukotrienes, which subsequently reduces leukocyte accumulation at the affected site. Furthermore, flavonoids inhibit lysosomal secretion, thereby limiting proliferation and exudation in the wound bed[39]. Saponins exhibit both anti-inflammatory and antibacterial properties by inhibiting the release of pro-inflammatory substances such as iNOS, IL, and TNF-α, leading to a decrease in exudate fluid and reduced vascular permeability. Steroids, by inhibiting phospholipase A2 enzyme and their ability to dissolve in lipids and proteins to form clumps on bacterial cell walls, function as effective antibacterial agents in wounds[40]. Lastly, tannins serve as astringents, precipitating proteins on the cell surface to reduce permeability, thereby aiding in pore closure, skin hardening, and the reduction of exudate and minor bleeding[41].

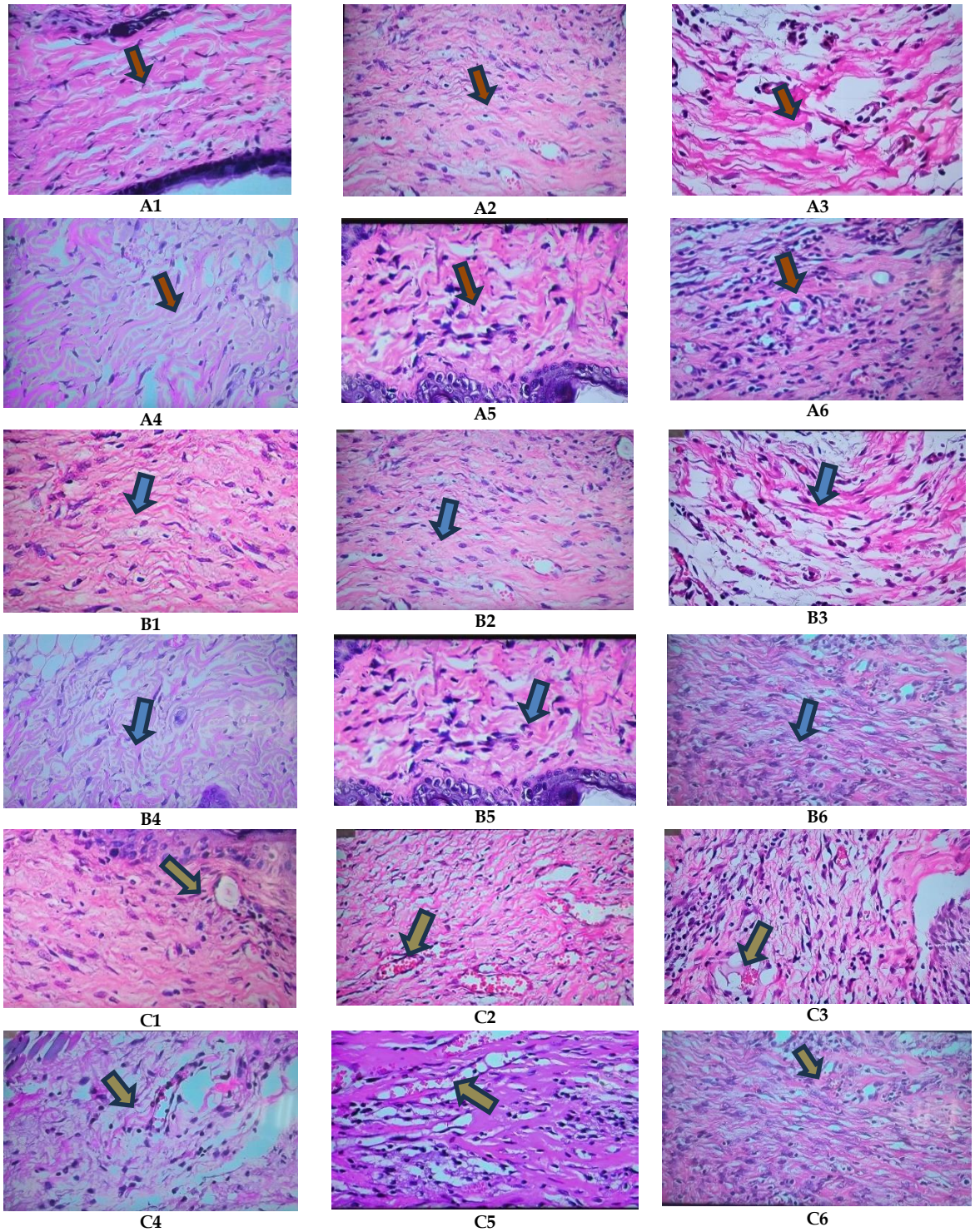

Figure 2. Histopathological description of rat skin after treatment. (**A**) red arrow: fibroblasts; **A1** (normal control); **A2** (Bioplacenton® positive control; **A3** (Formula 0); **A4** (Formula I (0.5% *R. pinnata* leaf extract nanoparticles); **A5** (Formula II (1% *R. pinnata* leaf extract nanoparticles); **A6** (Formula III (1.5% *R. pinnata* leaf extract nanoparticles). (**B**) blue arrow: collagen; **B1** (normal control); **B2** (Bioplacenton® positive control); **B3** (Formula 0); **B4** (Formula I (0.5% *R. pinnata* leaf extract nanoparticles); **B5** (Formula II (1% *R. pinnata* leaf extract nanoparticles); **B6** (Formula III (1.5% nanoparticles of *R. pinnata* leaf extract nanoparticles). (**C**) yellow arrow: angiogenesis; **C1** (normal control); **C2** (Bioplacenton® positive control); **C3** (Formula 0); B4 (Formula I (0.5% *R. pinnata* leaf extract nanoparticles); **C5** (Formula II (1% *R. pinnata* leaf extract nanoparticles); **C6** (Formula III (1.5% *R. pinnata* leaf extract nanoparticles).

CONCLUSION

This study successfully demonstrated the feasibility of formulating *R. pinnata* leaf extract into a nanoemulsion, characterized by a desirable particle size of 165.70 nm, a polydispersity index of 0.562, and a zeta potential of 22 mV. These nanometric

properties are crucial for enhanced penetration and efficacy. Importantly, the concentration of the extract within the nanoemulgel influenced critical physical properties such as organoleptic characteristics, pH, viscosity, and spreadability, yet remarkably maintained stability during freeze-thaw cycles and overall homogeneity. The resultant *R. pinnata* leaves extract nanoemulsion gel exhibited significant wound-healing activity, demonstrating a statistically significant difference ($p < 0.05$) compared to controls. Specifically, Formula III, containing 1.5% *R. pinnata* leaves extract nanoparticles, was the most effective formulation, achieving a remarkable 100% wound inhibition by day 14. Future investigations should focus on isolating, identifying, and quantifying the specific bioactive compounds within *R. pinnata* responsible for its promising wound healing and anti-inflammatory properties, further paving the way for its clinical application.

ACKNOWLEDGMENT

The author gratefully acknowledges the Faculty of Medicine and Health Sciences, Universitas Jambi, for their generous support through the applied research grant (contract number: 371/UN21.11/PT01.05/SPK/2021). This funding, sourced from the Faculty's Non-Tax State Revenue fund, was instrumental in facilitating the successful completion of this research.

AUTHORS' CONTRIBUTION

Conceptualization: Fathnur Sani Kasmadi, Ave Olivia Rahman, Havizur Rahman, Yuliawati, Agung Giri Samudra
Data curation: Fathnur Sani Kasmadi, Ave Olivia Rahman, Havizur Rahman, Yuliawati, Agung Giri Samudra
Formal analysis: Fathnur Sani Kasmadi, Ave Olivia Rahman, Havizur Rahman, Yuliawati, Agung Giri Samudra
Funding acquisition: Fathnur Sani Kasmadi
Investigation: Fathnur Sani Kasmadi
Methodology: Fathnur Sani Kasmadi, Ave Olivia Rahman, Havizur Rahman, Yuliawati, Agung Giri Samudra
Project administration: Fathnur Sani Kasmadi
Resources: Fathnur Sani Kasmadi, Ave Olivia Rahman, Havizur Rahman, Yuliawati
Software: -
Supervision: Fathnur Sani Kasmadi
Validation: Fathnur Sani Kasmadi
Visualization: Fathnur Sani Kasmadi
Writing - original draft: Fathnur Sani Kasmadi
Writing - review & editing: Fathnur Sani Kasmadi, Ave Olivia Rahman, Havizur Rahman, Yuliawati, Agung Giri Samudra

DATA AVAILABILITY

All data supporting the findings of this study are available from the corresponding author upon reasonable request.

CONFLICT OF INTEREST

The authors declare no conflicts of interest related to this study.

REFERENCES

1. Mathew-Steiner SS, Roy S, Sen CK. Collagen in wound healing. Bioengineering. 2021;8(5):63. DOI: 10.3390/bioengineering8050063; PMCID: PMC8151502; PMID: 34064689

2. Kasmadi FS, Rahman H, Rahman AO, Samudra AG, Floris C De. Incision wound healing test ethanolic extract gel from Ekor Naga (Rhaphidophora pinnata (L.f) Schott) leaves in white male rats. Pharmaciana. 2022;12(2):173-80. DOI: 10.12928/pharmaciana.v12i2.22825

3. Pan SP, Pirker T, Kunert O, Kretschmer N, Hummelbrunner S, Latkolik SL, et al. C13 megastigmane derivatives from epipremnum pinnatum: β-damascenone inhibits the expression of pro-inflammatory cytokines and leukocyte adhesion molecules as well as NF-κB signaling. Front Pharmacol. 2019;10:1351. DOI: 10.3389/fphar.2019.01351; PMCID: PMC6892967; PMID: 31849641

4. Tarigan BA, Kasmadi FS, Muhaimin. Topical anti-inflammatory effect of Ekor Naga (Rhaphidophora pinnata (L.f) Schott) leaves extract. Pharmaciana. 2021;11(3):303–11. DOI: 10.12928/pharmaciana.v11i3.17617

5. Khan I, Saeed K, Khan I. Nanoparticles: Properties, applications and toxicities. Arab J Chem. 2019;12(7):908-31. DOI: 10.1016/j.arabjc.2017.05.011

6. Sharma D, Kanchi S, Bisetty K. Biogenic synthesis of nanoparticles: A review. Arab J Chem. 2019;12(8):3576-600. DOI: 10.1016/j.arabjc.2015.11.002

7. Ansari SH, Islam F, Sameem M. Influence of nanotechnology on herbal drugs: A Review. J Adv Pharm Technol Res. 2012;3(3):142-6. DOI: 10.4103/2231-4040.101006; PMCID: PMC3459443; PMID: 23057000

8. Souto EB, Ribeiro AF, Ferreira MI, Teixeira MC, Shimojo AAM, Soriano JL, et al. New nanotechnologies for the treatment and repair of skin burns infections. Int J Mol Sci. 2020;21(2):393. DOI: 10.3390/ijms21020393; PMCID: 10.3390/ijms21020393; PMID: 31936277

9. Zeng C, Wei J, Persson MSM, Sarmanova A, Doherty M, Xie D, et al. Relative efficacy and safety of topical non-steroidal anti-inflammatory drugs for osteoarthritis: A systematic review and network meta-analysis of randomised controlled trials and observational studies. Br J Sports Med. 2018;52(10):642-50. DOI: 10.1136/bjsports-2017-098043; PMCID: PMC5931249; PMID: 29436380

10. Taha M, Alhakamy NA, Md S, Ahmad MZ, Rizwanullah M, Fatima S, et al. Nanogels as Potential Delivery Vehicles in Improving the Therapeutic Efficacy of Phytopharmaceuticals. Plymers. 2022;14(19):4141. DOI: 10.3390/polym14194141; PMCID: PMC9570606; PMID: 36236089

11. Samudra AG, Ramadhani N, Lestari G, Nugroho BH. Formulasi Nanopartikel Kitosan Ekstrak Metanol Alga Laut Coklat (Sargassum hystrix) dengan Metode Gelasi Ionik. J Ilmiah Manuntung. 2021;7(1):92–9. DOI: 10.51352/jim.v7i1.428

12. Samudra AG, Ramadhani N, Pertiwi R, Fitriani D, Sanik F, Burhan A. Antihyperglycemic activity of nanoemulsion of brown algae (Sargassum sp.). Ethanol extract in glucose tolerance test in male mice. Ann Pharm Fr. 2023;81(3):484-91. DOI: 10.1016/j.pharma.2022.11.011; PMID: 36464073

13. Saberi AH, Fang Y, McClements DJ. Effect of glycerol on formation, stability, and properties of vitamin-E enriched nanoemulsions produced using spontaneous emulsification. J Colloid Interface Sci. 2013;411:105-13. DOI: 10.1016/j.jcis.2013.08.041; PMID: 24050638

14. Bhatia S. Nanoparticles Types, Classification, Characterization, Fabrication Methods and Drug Delivery Applications. In: Natural Polymer Drug Delivery Systems. Cham; Springer: 2016. DOI: 10.1007/978-3-319-41129-3_2

15. Afrinanda R, Ristiawati Y, Islami MS, Pertiwi DV. Extraction, Identification, and Gel Formulation of Mangiferin from Mango (Mangifera indica L.) Leaves Extract. In: Hanani E, Permanasari ED, Sjahid LR, Dwita LP, Viviandhai D, Rindita, editors. Proceedings of the 1st Muhammadiyah International Conference on Health and Pharmaceutical Development MICH-PhD. Setúbal; SciTePress: 2019. DOI: 10.5220/0008240701380142

16. Builders P, Kabele-Toge B, Builders M, Chindo B, Anwunobi P, Isimi Y. Wound healing potential of formulated extract from hibiscus sabdariffa calyx. Indian J Pharm Sci. 2013;75(1):45-52. DOI: 10.4103/0250-474X.113549; PMCID: PMC3719149; PMID: 23901160

17. Shahtalebi MA, Asghari GR, Rahmani F, Shafiee F, Jahanian-Najafabadi A. Formulation of Herbal Gel of Antirrhinum majus Extract and Evaluation of its Anti- Propionibacterium acne Effects. Adv Biomed Res. 2018;7:53. DOI: 10.4103/abr.abr_99_17; PMCID: PMC5887696; PMID: 29657938

18. Darestani KD, Mirghazanfari SM, Moghaddam KG, Hejazi S. Leech therapy for linear incisional skin-wound healing in rats. J Acupunct Meridian Stud. 2014;7(4):194-201. DOI: 10.1016/j.jams.2014.01.001; PMID: 25151453

19. Wairata J, Fadlan A, Purnomo AS, Taher M, Ersam T. Total phenolic and flavonoid contents, antioxidant, antidiabetic and antiplasmodial activities of Garcinia forbesii King: A correlation study. Arab J Chem. 2022;15(2):103541. DOI: 10.1016/j.arabjc.2021.103541

20. Hidayah LA, Anggarani MA. Determination of Total Phenolic, Total Flavonoid, and Antioxidant Activity of India Onion Extract. Indones J Chem Sci. 2022;11(2):123-35. DOI: 10.15294/ijcs.v11i2.54610

21. Mizzi L, Chatzitzika C, Gatt R, Valdramidis V. HPLC analysis of phenolic compounds and flavonoids with overlapping peaks. Food Technol Biotechnol. 2020;58(1):12-9. DOI: 10.17113/ftb.58.01.20.6395

22. Li G, Ding K, Qiao Y, Zhang L, Zheng L, Pan T, et al. Flavonoids regulate inflammation and oxidative stress in cancer. Molecules. 2020;58(1):12-9. DOI: 10.3390/molecules25235628; PMCID: PMC7365340; PMID: 32684783

23. Hoang NH, Thanh T Le, Sangpueak R, Treekoon J, Saengchan C, Thepbandit W, et al. Chitosan Nanoparticles-Based Ionic Gelation Method: A Promising Candidate for Plant Disease Management. Polymers. 2022;14(4):662. DOI: 10.3390/polym14040662; PMCID: PMC8876194; PMID: 35215574

24. Bavel NV, Issler T, Pang L, Anikovskiy M, Prenner EJ. A Simple Method for Synthesis of Chitosan Nanoparticles with Ionic Gelation and Homogenization. Molecules. 2023;28(11):4328. DOI: 10.3390/molecules28114328; PMCID: PMC10254159; PMID: 37298804

25. Alehosseini E, Tabarestani HS, Kharazmi MS, Jafari SM. Physicochemical, Thermal, and Morphological Properties of Chitosan Nanoparticles Produced by Ionic Gelation. Foods. 2022;11(23):3841. DOI: 10.3390/foods11233841; PMCID: PMC9736386; PMID: 36496649

26. Popova EV, Zorin IM, Domnina NS, Novikova II, Krasnobaeva IL. Chitosan–Tripolyphosphate Nanoparticles: Synthesis by the Ionic Gelation Method, Properties, and Biological Activity. Russ J Gen Chem. 2020;90:1304-11. DOI: 10.1134/S1070363220070178

27. Hoshyar N, Gray S, Han H, Bao G. The effect of nanoparticle size on in vivo pharmacokinetics and cellular interaction. Nanomedicine. 2016;11(6):673-92. DOI: 10.2217/nnm.16.5; PMCID: PMC5561790; PMID: 27003448

28. Raval N, Maheshwari R, Kalyane D, Youngren-Ortiz SR, Chougule MB, Tekade RK. Importance of physicochemical characterization of nanoparticles in pharmaceutical product development. In: Tekade RK, editor. Basic Fundamentals of Drug Delivery. New York; Academic Press: 2019. p. 369-400. DOI: 10.1016/B978-0-12-817909-3.00010-8

29. Rahmat D, Farida Y, Brylianto AT, Sumarny R, Kumala S. Antidiabetic activity of nanoparticles containing Javanese turmeric rhizome extract: The strategy to change particle size. Int J Appl Pharm. 2020; 12(4):90-3. DOI: 10.22159/jap.2020v12i4.36249

30. Oudih SB, Tahtat D, Khodja AN, Mahlous M, Hammache Y, Guittoum AE, et al. Chitosan nanoparticles with controlled size and zeta potential. Polym Eng Sci. 2023;63(3):1011-21. DOI: 10.1002/pen.26261

31. Soleymanfallah S, Khoshkhoo Z, Hosseini SE, Azizi MH. Preparation, physical properties, and evaluation of antioxidant capacity of aqueous grape extract loaded in chitosan-TPP nanoparticles. Food Sci Nutr. 2022;10(10):3272-81. DOI: 10.1002/fsn3.2891

32. Virk P, Awad MA, Saleh Abdu-llah Alsaif S, Hendi AA, Elobeid M, Ortashi K, et al. Green synthesis of Moringa oleifera leaf nanoparticles and an assessment of their therapeutic potential. J King Saud Univ Sci. 2023;35(3):102576. DOI: 10.1016/j.jksus.2023.102576

33. Bhatia S, Shah YA, Al-Harassi A, Jawad M, Khan TS, Koca E, et al. Tuning the structure and physiochemical properties of sodium alginate and chitosan composite films through sodium tripolyphosphate (STPP) crosslinking. Int J Biol Macromol. 2024;264(Pt 2):130463. DOI: 10.1016/j.ijbiomac.2024.130463; PMID: 38423442

34. Oryan A, Mohammadalipour A, Moshiri A, Tabandeh MR. Topical application of aloe vera accelerated wound healing, modeling, and remodeling. Ann Plast Surg. 2016;77(1):37–46. DOI: 10.1097/SAP.0000000000000239; PMID: 25003428

35. Loo HL, Goh BH, Lee LH, Chuah LH. Application of chitosan-based nanoparticles in skin wound healing. Asian J Pharm Sci. 2022;17(3):299-332. DOI: 10.1016/j.ajps.2022.04.001

36. Hajialyani M, Tewari D, Sobarzo-Sánchez E, Nabavi SM, Farzaei MH, Abdollahi M. Natural product-based nanomedicines for wound healing purposes: therapeutic targets and drug delivery systems. Int J Nanomedicine. 2018;13:5023-43. DOI: 10.2147/ijn.s174072; PMCID: PMC6128268; PMID: 30214204

37. Thakur R, Jain N, Pathak R, Sandhu SS. Practices in wound healing studies of plants. Evid Based Complement Alternat Med. 2011:2011:438056. DOI: 10.1155/2011/438056; PMCID: PMC3118986; PMID: 21716711

38. Schilrreff P, Alexiev U. Chronic Inflammation in Non-Healing Skin Wounds and Promising Natural Bioactive Compounds Treatment. Int J Mol Sci. 2022;23(9):4928. DOI: 10.3390/ijms23094928; PMCID: PMC9104327; PMID: 35563319

39. Deka B, Bhattacharjee B, Shakya A, Ikbal AMA, Goswami C, Sarma S. Mechanism of Action of Wound Healing Activity of Calendula officinalis: A Comprehensive Review. Pharm Biosci J. 2021;9(1):28-44. DOI: 10.20510/ukjpb/9/i1/1609684673

40. Razika L, Thanina AC, Nadjiba CM, Narimen B, Mahdi DM, Karim A. Antioxidant and wound healing potential of saponins extracted from the leaves of Algerian Urtica dioica L. Pak J Pharm Sci. 2017;30(3(Suppl.)):1023-9. PMID: 28655702

41. Ambreen M, Mirza SA. Evaluation of anti-inflammatory and wound healing potential of tannins isolated from leaf callus cultures of Achyranthes aspera and Ocimum basilicum. Pak J Pharm Sci. 2020;33(1(Supplementary)):361-9. PMID: 32122869